Identifying target properties for the design of meta-material tank track pads

V.S. Dangeti, Z.T. Satterfield, G. Fadel, G. Li, & N. Coutris
Clemson University, Clemson, SC, USA

M. P. Castanier, D. Ostberg
US Army TARDEC, Warren, MI, USA

ABSTRACT: This work presents a methodology to design an alternate meta-material that can provide some of the desired properties of tank track pads while eliminating or reducing the hysteresis losses of elastomer. To determine the requirements for linear elastic meta-materials, dynamic analyses of a rollover event are conducted on a simplified but representative finite element model of a backer pad. From these analyses, the complex dependence of the strain history on different strain components is elucidated. Due to the nonlinearity of elastomers, tangent stiffness matrices are required to update the stress states at different strain increments. The elasticity tensors (tangent operators) determined at a set of strain levels, are used as prescribed constitutive parameters to tailor the meta-material unit-cell topology. The optimal material properties according to which the track pad is designed with linear elastic meta-material are identified. A topology optimization study to target these material properties is ongoing.

1 TANK TRACK PAD SYSTEMS

The U.S. Army employs the M1 Abrams tank as a tactical asset in combat and peace operations. Rubber pads are installed on the tracks for traction and road protection. Wear life and fatigue failure are common issues with these pads. The system and issues are detailed in the following section.

1.1 *Physical System*

The M1 Abrams tank uses the T158LL track pad to provide traction, dampen sound, and protect road surfaces [1]. The track backer pad consists of a homogeneous rubber pad bonded to a steel backing plate, as shown in Figure 1 from Ref. [2]. The current material that is used to manufacture the T158LL tank track pads is a carbon-black-filled Styrene-Butadiene Rubber (SBR) [2]. The use of carbon black reinforcements improves strength and abrasion resistance of SBR [3].

Figure 1. T158LL Track Pad [2]

1.2 *Limits to rubber track pads*

The service life of these rubber backer pads is approximately 2000 miles over a distribution of paved roads, gravel, and off-road terrain. The costs associated with the repairs and replacements of backer pads are very high. Therefore, increasing the durability of these pads could significantly reduce maintenance costs and increase vehicle availability.

During sustained operation, there is heating and a subsequent loss of strength of the rubber material due to hysteretic heat loss. The cyclic compressive loading of the track pad causes this hysteretic loss as shown in Figure 2 (left). The heat generated from

Report Documentation Page

Form Approved
OMB No. 0704-0188

1. REPORT DATE	2. REPORT TYPE	3. DATES COVERED
05 MAR 2014	**Journal Article**	**07-10-2013 to 07-02-2014**

4. TITLE AND SUBTITLE	5a. CONTRACT NUMBER
Identifying target properties for the design of meta-material tank track pads	**W56HZV-14-2-0001**
	5b. GRANT NUMBER
	5c. PROGRAM ELEMENT NUMBER
6. AUTHOR(S)	5d. PROJECT NUMBER
V Dangeti; Z Satterfield; G Fadel; G Li; N Coutris	5e. TASK NUMBER
	5f. WORK UNIT NUMBER
7. PERFORMING ORGANIZATION NAME(S) AND ADDRESS(ES)	8. PERFORMING ORGANIZATION REPORT NUMBER
Clemson University,201 Sikes Hall,Clemson,SC,29634	**; #25268**
9. SPONSORING/MONITORING AGENCY NAME(S) AND ADDRESS(ES)	10. SPONSOR/MONITOR'S ACRONYM(S)
U.S. Army TARDEC, 6501 East Eleven Mile Rd, Warren, Mi, 48397-5000	**TARDEC**
	11. SPONSOR/MONITOR'S REPORT NUMBER(S)
	#25268

12. DISTRIBUTION/AVAILABILITY STATEMENT

Approved for public release; distribution unlimited

13. SUPPLEMENTARY NOTES

14. ABSTRACT

This work presents a methodology to design an alternate meta-material that can provide some of the desired properties of tank track pads while eliminating or reducing the hysteresis losses of elastomer. To determine the requirements for linear elastic meta-materials, dynamic analyses of a rollover event are conducted on a simplified but representative finite element model of a backer pad. From these analyses, the complex dependence of the strain history on different strain components is elucidated. Due to the nonlinearity of elastomers, tangent stiffness matrices are required to update the stress states at different strain increments. The elasticity tensors (tangent operators) determined at a set of strain levels, are used as prescribed constitutive parameters to tailor the meta-material unit-cell topology. The optimal material properties according to which the track pad is designed with linear elastic meta-material are identified. A topology optimization study to target these material properties is ongoing.

15. SUBJECT TERMS

16. SECURITY CLASSIFICATION OF:			17. LIMITATION OF ABSTRACT	18. NUMBER OF PAGES	19a. NAME OF RESPONSIBLE PERSON
a. REPORT	b. ABSTRACT	c. THIS PAGE			
unclassified	**unclassified**	**unclassified**	**Public Release**	**6**	

hysteretic loss and other friction can exceed 150°C during high-speed operation [4].

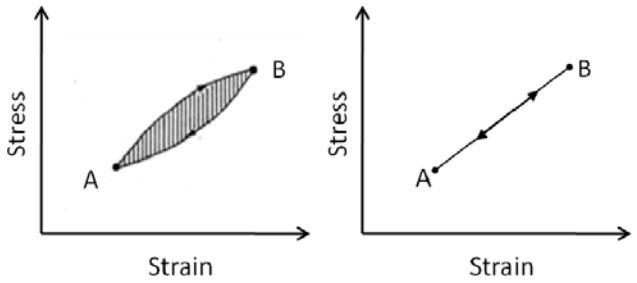

Figure 2. Viscoelastic material with hysteretic loss (left) [5] and linear elastic material without hysteretic loss (right)

Elastomers have the desired compliance required to provide traction and sound dampening since they exhibit high strains at low stress levels. However, elastomers demonstrate hysteretic loss due to their viscoelastic nature. Therefore, a new material is sought to achieve high compliance while reducing or eliminating hysteretic heat loss. This research explores a methodology to design an alternate material that can still provide the desired properties of the current track pads while improving their structural performance under extreme loading conditions.

2 MOTIVATION

In the current research, we propose to significantly reduce and possibly eliminate the hysteretic losses associated with the backer pad by using linear elastic materials, which are inherently non-hysteretic as shown in Figure 2 (right). However, the elastic modulus of elastomeric materials generally lies between 2MPa and 20MPa, which is several orders of magnitude less than that of linear elastic materials such as aluminum, titanium, or steel.

A need exists to create a material that fills the void in the Ashby chart [6] shown in Figure 3. The new material would need to exhibit a low loss coefficient and low elastic modulus. Since traditional materials do not fill this void, a meta-material must be created. In general, a meta-material is defined as an engineered material with exceptional properties usually not encountered in nature [7]. We would like to adapt this definition to our need: a meta-material is a material system whose geometric or topological structure is such that the behavior of the system matches a desired one and is significantly different from the properties of the bulk material used [8]. The material parameters such as elastic moduli and Poisson's ratio of a linear elastic material, which lead to the behavior depicted by the meta-material region described in the Ashby chart, need to be determined. The focus of this paper is on a methodology to determine the meta-material requirements for a track pad with low hysteresis loss and high durability.

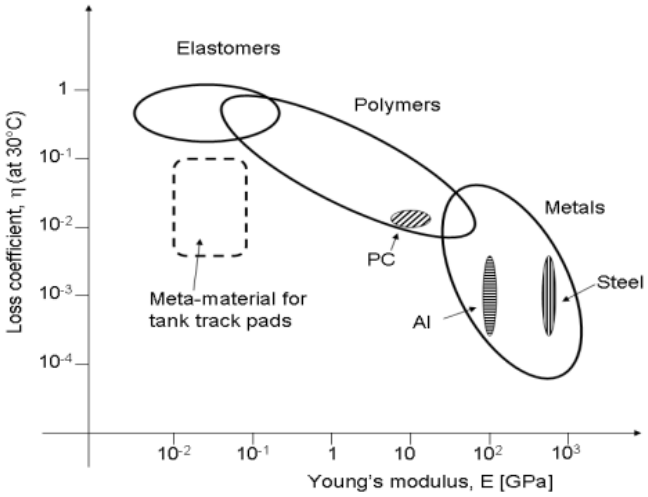

Figure 3. Ashby chart [6]: meta-material characterization

3 FINITE ELEMENT ANALYSIS (FEA)

For the present analysis, a 2nd order Ogden Hyperelastic material model is used to represent the elastomer's stress-strain behavior. The Ogden model strain energy potential is expressed in terms of the principal stretches which is an advantage because they are directly related to the principal strains. An accurate representation of the characteristic stress-strain curves was achieved using the 2nd order Ogden model in [2]. The resulting fit is shown in Figure 4, and the material parameters derived from the fitting process are shown in Table 1.

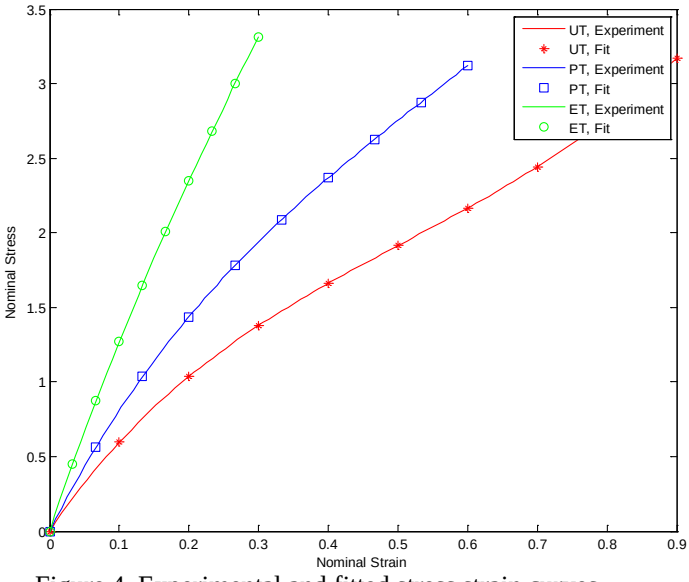

Figure 4. Experimental and fitted stress strain curves

Table 1. Elastomer material properties

Part	Material model	Properties
Track Pads	2nd Order Ogden Hyperelastic	μ_1 = 2.275319 MPa μ_2 = 0.054452 MPa α_1 = -1.00837 α_2 = 7.863497

A simplified but representative model of a backer pad developed under a previous research study [2], which is shown in Figure 5, was used as a numerical example. Dynamic FEA simulations were conducted to extract the stress-strain response during a single rollover event. Abaqus/CAE 6.10, a commercial FEA tool, was used to investigate the dynamic response of the backer pad.

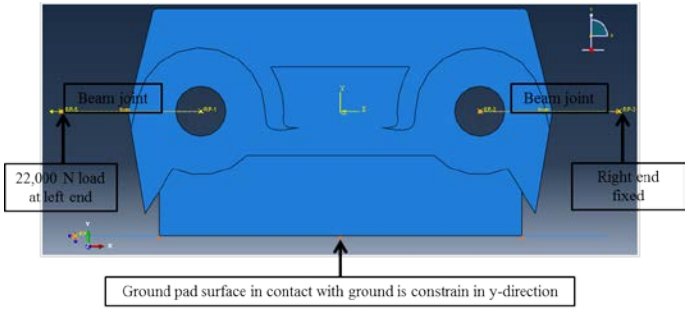

Figure 5. Loading and boundary conditions on track pad

The track assembly is assumed to be resting on flat ground, which is represented as a rigid analytical surface. The rigid surface is constrained in all (three rotational and three translational) degrees of freedom. In this simulation only one track pad is modeled. A constraint on the vertical degree of freedom is applied on the lower surface of the ground pad. The links between track pad sub-assemblies are represented via solid beams. To simulate tension in the track assembly, the right end of the assembly (RP-3) is kept fixed while at the other end (RP-5), a load of 22,000 N in the negative x-direction is applied [2]. Figure 5 shows the boundary conditions and loads on the track pad. The dynamic load experienced by the track pad is simulated by applying 35,000N load to the road wheel spindle, and by applying a linear velocity of 70km/hr as shown in Figure 6. An angular velocity of 10rev/s is also applied to the road wheel spindle.

In Figure 7, contours of maximum principal strain are plotted at different times as the rolling road wheel loads the backer pad. It is shown that at time t = 0.010 seconds, the road wheel deforms the backer pad fully, causing maximum deformation on the top of the left beam joint. The beam joint is protected by the much stiffer steel plate onto which the backer pad is bonded. Since the road wheel is rotating at a high speed and a friction formulation is applied in the surface contact, the backer pad material also deforms in shear combined with compression. The shearing effect can be observed at the left side of the backer pad which is slightly at an angle when not deformed. Under full deformation the same side is curved and moves to the left (t=0.014s).

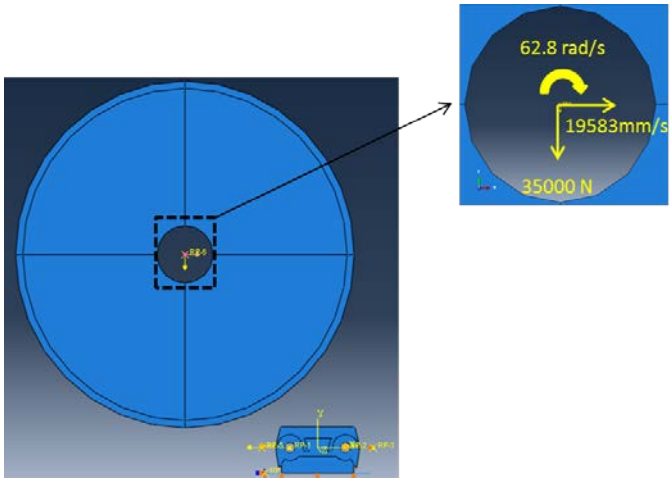

Figure 6. Loading conditions on road wheel

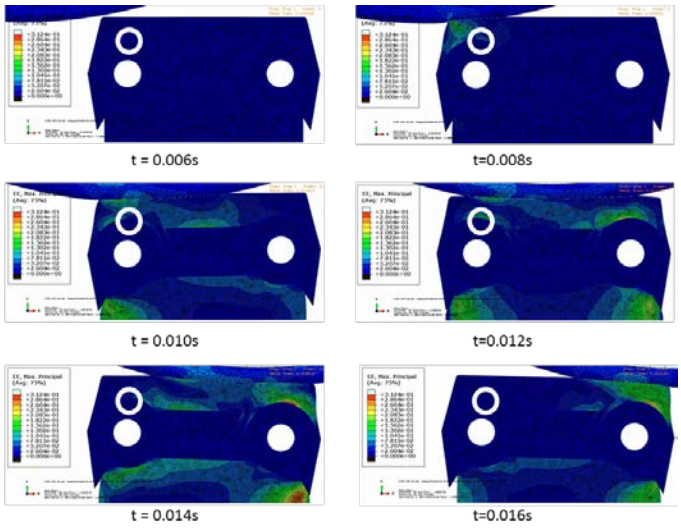

Figure 7. Maximum principal strain contour plots on backer pad at different times and the area with shortest fatigue life circle circled in white.

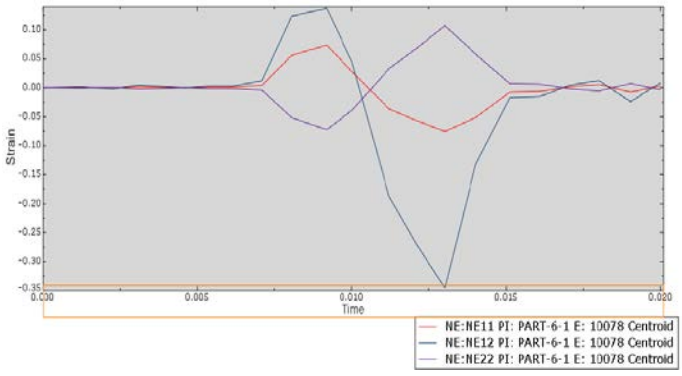

Figure 8. History of nominal strain components during backer pad rollover event, at the point of shortest life

For illustrative purposes, Figure 8 displays the strain history recovered from an element present in the area with shortest fatigue life. This area was

recognized by fatigue damage analysis conducted in [2] and is depicted by the circled region in Figure 6. The strain history exhibits a complex dependence on all the three strain components with time. The component of the strain in y-axis (NE22) shows major compression events at 0.008s and 0.012s with a corresponding coupled response in tension and shear. As observed from the analysis, the maximum strain occurs by shear due to the compressive force exerted by the road wheel.

The strain history in Figure 8 shows a shear strain that is approximately three times the strain due to compression. Due to the highly dynamic nature of road wheel, the strain history varies depending on where the road wheel strikes the track pad. The strain history is also different for different elements in the backer pad or ground pad. Regardless of where the road wheel strikes the track pad, the strain history is complex in all regions and under all conditions and depends on all three components of strain. Therefore, the challenge is to estimate the cumulative effects of these strain histories and derive requirements for a meta-material to target this complex strain response.

4 REQUIREMENTS DETERMINATION

As described in Section 3, the strain history has a complex dependence on all three strain components, and the mode of failure of the track pad is not due to a single loading stress case such as the compressive stress due to the weight of the tank. Therefore, multiple load scenarios must be taken into consideration while designing the approach to determine meta-material requirements.

The approach presented in the following section considers certain modes of deformation that put the material into a particular state of strain. The main objective is to achieve "pure" states of strain such that the stress-strain curve represents the elastomer behavior only in the desired state of stress. Therefore, the material response in each case will not have a complex dependency on other strain components. This enables the determination of the requirements of a meta-material in the form of stiffness matrices for the particular state of strain. The stiffness matrices determined at the set of strain levels may be used as constitutive parameters by the topology optimizer to tailor the meta-material unit-cell.

The approach is based on tangent elasticity tensors for hyperelastic material models [9]. The free energy density for the Ogden Hyperelastic material model is given by,

$$\psi = \sum_{k=1}^{K} \frac{\mu_k}{\alpha_k}\left[\bar{\lambda}_1^{\alpha_k} + \bar{\lambda}_2^{\alpha_k} + \bar{\lambda}_3^{\alpha_k} - 3\right] + k(J-1)^2$$

where $\bar{\lambda}_i = J^{-1/3}\lambda_i$, $\lambda_i, i = 1,2,3$ are the three principal stretches. $J = \lambda_1\lambda_2\lambda_3$, is the volume ratio. μ_k, α_k are material fitting parameters given in Table 1. k is the bulk modulus which is taken as 1 GPa in this study. A fourth-order elasticity tensor (tangent operator) may be introduced such that the changes in stress $\Delta\boldsymbol{S}$, caused by the changes in deformation $\Delta\boldsymbol{C}$, can be described via,

$$\Delta\boldsymbol{S} = \mathbb{C} : \frac{1}{2}\Delta\boldsymbol{C}$$

where S is the second Piola-Kirchhoff stress tensor and C is the right Cauchy-Green deformation tensor. The tangent elasticity tensor can now be described in terms of the free energy density, second Piola-Kirchhoff stress tensor and Cauchy-Green strain tensor as,

$$\boldsymbol{S} = 2\frac{\partial\psi}{\partial\boldsymbol{C}},\ \mathbb{C} = 2\frac{\partial\boldsymbol{S}}{\partial\boldsymbol{C}} = 4\frac{\partial^2\psi}{\partial\boldsymbol{C}^2}$$

When calculating, the tangent elasticity tensors for nearly-incompressible materials, the stress tensor and corresponding tangent elasticity tensor may be divided into isochoric and volumetric forms.

$$\boldsymbol{S} = \boldsymbol{S}_{iso} + \boldsymbol{S}_{\boldsymbol{vol}}$$

The isochoric part of the 2nd Piola-Kirchhoff stress tensor is given by,

$$S_{iso}^{i} = J^{-2/3}\left[\sum_{k=1}^{K}\mu_k\bar{\lambda}_i^{\alpha_k-2} - \sum_{j=1}^{3}\sum_{k=1}^{3}\frac{\mu_k}{3}\frac{\bar{\lambda}_j^{\alpha_k}}{\bar{\lambda}_i^2}\right], \quad i = 1,2,3$$

$$\boldsymbol{S}_{iso} = \sum_{\boldsymbol{i=1}}^{\boldsymbol{3}} S_{iso}^{i}\ \boldsymbol{N_i} \otimes \boldsymbol{N_i}$$

Where, N_i are the eigenvectors of the Cauchy-Green tensor. The volumetric part of the 2nd Piola-Kirchhoff stress tensor is given by,

$$\boldsymbol{S}_{\boldsymbol{vol}} = 2k(J-1)J\boldsymbol{C}^{-1}$$

The corresponding tangent elasticity tensor is given by,

$$\mathbb{C} = \mathbb{C}_{iso} + \mathbb{C}_{vol}$$

$$\mathbb{C}_{iso} = \sum_{i,j=1}^{3} \frac{1}{\lambda_j}\frac{\partial S_{iso}^{i}}{\partial \lambda_j} \boldsymbol{N}_i \otimes \boldsymbol{N}_i \otimes \boldsymbol{N}_j \otimes \boldsymbol{N}_j + \sum_{\substack{i,j=1 \\ i\neq j}}^{3} \frac{S_{iso}^{j} - S_{iso}^{i}}{\lambda_j^2 - \lambda_i^2} \begin{bmatrix} \boldsymbol{N}_i \otimes \boldsymbol{N}_j \otimes \boldsymbol{N}_i \otimes \boldsymbol{N}_j \\ + \boldsymbol{N}_i \otimes \boldsymbol{N}_j \otimes \boldsymbol{N}_j \otimes \boldsymbol{N}_i \end{bmatrix}$$

$$\mathbb{C}_{vol} = [2k(2J-1)J]\,\boldsymbol{C}^{-1} \otimes \boldsymbol{C}^{-1} - 2k(J-1)J\boldsymbol{C}^{-1} \odot \boldsymbol{C}^{-1}$$

The tangent operators determined at a set of strain levels for pure stress states can now be used as constitutive parametric targets for the meta-material unit-cell topology optimization.

$$[\Delta \boldsymbol{S}] = \begin{bmatrix} \mathbb{C}_{11} & \mathbb{C}_{12} & \mathbb{C}_{13} & 0 & 0 & 0 \\ \mathbb{C}_{12} & \mathbb{C}_{22} & \mathbb{C}_{23} & 0 & 0 & 0 \\ \mathbb{C}_{13} & \mathbb{C}_{23} & \mathbb{C}_{33} & 0 & 0 & 0 \\ 0 & 0 & 0 & \mathbb{C}_{44} & 0 & 0 \\ 0 & 0 & 0 & 0 & \mathbb{C}_{55} & 0 \\ 0 & 0 & 0 & 0 & 0 & \mathbb{C}_{66} \end{bmatrix} \left[\frac{1}{2}\Delta \boldsymbol{C}\right]$$

The tangent operators for each strain level at different characteristic stress states were calculated and are shown in Table 2.

Table 2. Results of tangent operaters at each strain level (units: MPa)

Stress State	λ	$\mathbb{C}_{11}$	$\mathbb{C}_{22}$	$\mathbb{C}_{33}$	$\mathbb{C}_{44}$	$\mathbb{C}_{55}$	$\mathbb{C}_{66}$	$\mathbb{C}_{12}$	$\mathbb{C}_{23}$	$\mathbb{C}_{13}$
Uniaxial Tension	1.1	1367.64	2424.11	2424.11	1.80	1.92	1.80	1817.21	2418.24	1817.21
	1.2	965.36	2885.31	2885.31	1.42	2.35	1.42	1666.11	2878.05	1666.11
	1.3	700.71	3386.74	3386.74	1.15	2.86	1.15	1538.19	3377.89	1538.19
	1.4	520.88	3928.45	3928.45	0.95	3.47	0.95	1428.49	3917.84	1428.49
	1.5	395.24	4510.63	4510.63	0.81	4.21	0.81	1333.35	4497.96	1333.35
	1.6	305.33	5133.22	5133.22	0.69	5.13	0.69	1250.04	5118.43	1250.04
	1.7	236.64	5796.67	5796.67	0.62	6.34	0.62	1176.44	5779.47	1176.44
Equi-biaxial Tension	1.1	1368.10	1368.10	4295.28	0.08	2.19	2.19	1367.03	2419.05	2419.05
	1.2	965.99	965.99	8608.12	-0.61	2.04	2.04	966.66	2879.92	2879.92
	1.3	701.40	701.40	16326.95	-0.93	1.90	1.90	702.89	3381.12	3381.12
Pure Shear	1.1	1367.79	2003.55	2932.30	1.31	2.66	1.92	1652.82	1998.87	2418.52
	1.2	965.57	2003.96	4152.48	0.63	3.01	1.61	1389.77	1999.23	2878.70
	1.3	700.94	2004.36	5718.67	0.17	3.38	1.36	1184.94	1999.53	3379.03
	1.4	521.10	2004.79	7691.52	-0.15	3.75	1.17	1022.32	1999.75	3919.59
	1.5	395.45	2005.30	10135.33	-0.36	4.13	1.02	891.06	1999.87	4500.47

5 CONCLUSIONS & FUTURE WORK

In this paper, the design of a meta-material that can provide some of the desired properties of tank track pads while eliminating or reducing the hysteresis losses of elastomer was explored. To determine the performance requirements, dynamic analyses of a rollover event were conducted on a simplified but representative finite element model of a backer pad. From these analyses, the complex dependence of the strain history on different strain components was observed. Tangent stiffness matrices were derived to update the stress states at different strain increments. The tangent elasticity tensors determined at a set of strain levels were used as prescribed constitutive parameters to tailor the meta-material unit-cell topology. Then, the optimal material properties for the linear elastic meta-material were identified.

The tangent elasticity tensors determined in this work were only for "pure" stress states. However, the methodology described can be utilized directly to obtain tangent operators from strain tensor determined using 3D FEA models. 3D FEA models simulating complex failure modes, effects of localized tensile stresses and effects of terrain and more realistic "off-road" simulations will be considered as case studies in future work.

A topology optimization study to target the optimal material properties identified in this paper is ongoing. The optimization approach that has been adopted is briefly summarized as follows. Because the strain history has a complex dependence on all three strain components, the ideal unit-cell topology must mimic the material behavior of the elastomer in all the "pure" stress scenarios which characterize the elastomer behavior i.e. uniaxial tension, planar tension (or pure shear) and equibiaxial tension. Therefore, the optimization formulation must consider all the three strain components simultaneously, leading to a very difficult case where there are a high number of objective functions to satisfy. The multi-objective formulation at each strain level can be given as follows,

Objectives:

a. Minimize (metaNE11 – sbrNE11)^2
b. Minimize (metaNE22 – sbrNE22)^2
c. Minimize (metaNE12 – sbrNE12)^2

where metaNEij and sbrNEij are the nominal strains of the meta-material and elastomer respectively. The topology must be optimized so as to satisfy the relation $\Delta S = \mathbb{C} : \frac{1}{2} \Delta C$ where the design targets in each case would be the 9 tangent operators, $\mathbb{C}_{11}$, $\mathbb{C}_{22}$, $\mathbb{C}_{33}$, $\mathbb{C}_{44}$, $\mathbb{C}_{55}$, $\mathbb{C}_{66}$, $\mathbb{C}_{12}$, $\mathbb{C}_{23}$, and $\mathbb{C}_{13}$ for the particular strain level.

The solution of the optimization problems will be considered in future work.

6 DISCLAIMER

Reference herein to any specific commercial company, product, process, or service by trade name, trademark, manufacturer, or otherwise, does not necessarily constitute or imply its endorsement, recommendation, or favoring by the United States Government or the Department of the Army (DoA). The opinions of the authors expressed herein do not necessarily state or reflect those of the United States Government or the DoA, and shall not be used for advertising or product endorsement purposes.

7 DISTRIBUTION STATEMENT

UNCLASSIFIED: Distribution A. Approved for public release.

8 ACKNOWLEDGMENT

This work was partially supported by the Automotive Research Center (ARC), a US Army Center of Excellence for modeling and simulation of ground vehicles.

9 REFERENCES

[1] National Materials Advisory Board, “Elastomers for Tank-Track Pads”, National Academy Press, Washington D.C., 1982.

[2] Mars, W., V., Ostberg, D., “Fatigue Damage Analysis of an Elastomeric Tank track component”, *SIMULIA Community Conference*, 2012.

[3] Gogos, A., N., et al, “A Study of Elastomeric Materials for Tank Track Pads”, New Jersey, 1978.

[4] Ostberg, D., Bradford, B., “Impact of Loading of Abrams Suspension on Track Performance and Durability”, *Proceedings of 2009 Ground Vehicle Systems Engineering and Technology (GVSETS)*, 2009.

[5] Clark, S. K., Dodge, R. N., “A Handbook for Rolling Resistance of Pneumatic Tires,” *Industrial Development Division, Institute of Science and Technology*, 1979.

[6] Ashby, M. F., “Materials Selection in Mechanical Design,” Elsevier Ltd., 2012.

[7] Sigmund, O., “Systematic Design of Meta-Materials by Topology Optimization,” IUTAM Symposium on Modeling Nanomaterials and Nanosystems, Springer, 2009.

[8] Day, J., “Equibiaxial Stretching of Elastomeric Sheets, An Analytical Verification of Experimental Technique,” Axel Products Testing and Analysis, 1999.

[9] Steinmann, P., et al “Hyperelastic Models for Rubber-like Materials: Consistent Tangent Operators for Suitability for Treolar’s Data”, *Archive of Applied Mechanics*, 2012.